SLOW WALKER2, a NOC1/MAK21 Homologue, Is Essential for Coordinated Cell Cycle Progression during Female Gametophyte Development in Arabidopsis[1[C][OA]]

Na Li[2], Li Yuan[2], Naiyou Liu, Dongqiao Shi, Xinran Li, Zuoshun Tang, Jie Liu, Venkatesan Sundaresan, and Wei-Cai Yang*

Key Laboratory of Molecular and Developmental Biology, Institute of Genetics and Developmental Biology, Chinese Academy of Sciences, Beijing 100101, China (N.Li, L.Y., N.Liu, D.S., X.L., Z.T., J.L., W.-C.Y.); Graduate University of Chinese Academy of Sciences, Beijing, 100039, China (N.Li, L.Y., N.Liu); and Plant Biology and Agronomy, Life Sciences Addition 1002, University of California, Davis, California 95616 (V.S.)

Morphogenesis requires the coordination of cell growth, division, and cell differentiation. Female gametogenesis in flowering plants, where a single haploid spore undergoes continuous growth and nuclear division without cytokinesis to form an eight-nucleate coenocytic embryo sac before cellularization, provides a good system to study the genetic control of such processes in multicellular organisms. Here, we report the characterization of an Arabidopsis (*Arabidopsis thaliana*) female gametophyte mutant, *slow walker2* (*swa2*), in which the progression of the mitotic cycles and the synchrony of female gametophyte development were impaired, causing an arrest of female gametophytes at the two-, four-, or eight-nucleate stage. Delayed pollination test showed that a portion of the mutant ovules were able to develop into functional embryo sacs and could be fertilized. *SWA2* encodes a nucleolar protein homologous to yeast NUCLEOLAR COMPLEX ASSOCIATED PROTEIN1 (NOC1)/MAINTENANCE OF KILLER21 that, together with NOC2, is involved in preribosome export from the nucleus to the cytoplasm. Similarly, SWA2 can physically interact with a putative Arabidopsis NOC2 homologue. *SWA2* is expressed ubiquitously throughout the plant, at high levels in actively dividing tissues and gametophytes. Therefore, we conclude that SWA2 most likely plays a role in ribosome biogenesis that is essential for the coordinated mitotic progression of the female gametophyte.

Morphogenesis requires tightly coordinated coupling of cellular activities, such as cell growth, cell division, and differentiation. In past decades, significant progress on cell cycle control has been achieved mostly in single-celled organisms and cultured mammalian cells. The elucidation of the cyclin/cyclin-dependent kinase checkpoint control, for example, provides insight into molecular mechanisms on how and when cells divide. Mechanisms coupling cell growth to environmental and developmental signals have also been investigated. Ribosome biogenesis, a key for rapid cell growth, is coupled with nutrient availability and stress signals via the TOR signaling pathway (Warner et al., 2001; Wullischleger et al., 2006). However, questions such as how the cell senses intrinsic cellular homeostatic signals remain to be addressed. For example, how ribosome dynamics and translational activities are measured and coupled to cytokinesis and cell differentiation, especially in the context of development of multicellular organisms.

Female gametogenesis in Arabidopsis (*Arabidopsis thaliana*) is a unique system to address such questions in multicellular organisms. During female gametogenesis, the haploid functional megaspore undergoes continuous cell growth and three cycles of consecutive nuclear division without cytokinesis, giving rise to a giant eight-nucleate, coenocytic cell: the embryo sac. The size of the embryo sac increases about 6-fold without cytokinesis until it reaches its maximum during gametogenesis in maize (*Zea mays*; Dow and Mascarenhas, 1991). The two polar nuclei migrate toward the micropylar half of the embryo sac and eventually fuse to give rise to a diploid nucleus of the central cell. As the polar nuclei migrate, cellularization takes place simultaneously to divide the coenocytic embryo sac into seven cells of four cell fates: three antipodal cells, two synergid cells, one egg cell, and one central cell (Drews et al., 1998; Grossniklaus and Schneitz, 1998; Yang and Sundaresan, 2000; Wilson

[1] This work was supported by the Ministry of Science and Technology (grant no. 2007CB108702), the National Science Foundation of China (grant no. 30830063), and the State Key Laboratory of Crop Biology at Shandong Agricultural University, China.

[2] These authors contributed equally to the article.

* Corresponding author; e-mail wcyang@genetics.ac.cn.

The author responsible for distribution of materials integral to the findings presented in this article in accordance with the policy described in the Instructions for Authors (www.plantphysiol.org) is: Wei-Cai Yang (wcyang@genetics.ac.cn).

[C] Some figures in this article are displayed in color online but in black and white in the print edition.

[OA] Open Access articles can be viewed online without a subscription.

www.plantphysiol.org/cgi/doi/10.1104/pp.109.142414

and Yang, 2004). Obviously, its haploid nature and coupling of cell growth, division, and cell fates make the female gametophyte a nice system to investigate how these cellular activities are coordinated in development.

The temporal and spatial control of cell growth, the mitotic division cycles, and cell fate specification during female gametogenesis have been the focus of sexual plant reproduction research. Recently, genetic studies have identified gametophytic mutations that start to shed light on the genetic and molecular control of these processes. Mutations in genes involved in diverse cellular functions, including *ANDARTA* (Howden et al., 1998), *GAMETOPHYTIC FACTOR1* (*GFA1*; Christensen et al., 1997), *HADAD* (Moore et al., 1997), *LETHAL OVULE2* (Sheridan and Huang, 1997), *LYSOPHOSPHATIDYL ACYLTRANSFERASE* (Kim et al., 2005), *NOMEGA* (Kwee and Sundaresan, 2003), *PROLIFERA* (Springer et al., 1995), *SLOW WALKER1* (*SWA1*; Shi et al., 2005), *SUCCINATE DEHYDROGENASE* (Leon et al., 2007), and *TISTRYA* (Howden et al., 1998), all result in defective gametophytic cell divisions, implying that progression of the mitotic cycle is critical for the formation of a functional female gametophyte. Loss-of-function mutations in the Arabidopsis *RETINOBLASTOMA-RELATED PROTEIN1*, a key negative regulator controlling the G1/S transition of the cell cycle, result in uncontrolled nuclear proliferation and cell fates, giving rise to embryo sacs with supernumerary nuclei that are irregular in size and partially enclosed by cell wall-like structures (Ebel et al., 2004). Loss of functions in *CYTOKININ INDEPENDENT1* (Hejatko et al., 2003), *DIANA/AGAMOUS-LIKE61* (Bemer et al., 2008), *AGAMOUS-LIKE80* (Portereiko et al., 2006a), and *NUCLEAR FUSION DEFECTIVE1* (Portereiko et al., 2006b) affect polar nuclear fusion and central cell development.

Accumulating data suggest a key role of the nucleolus in cell survival and proliferation (Cockell and Gasser, 1999; Shaw and Doonan, 2005). A number of nucleolar proteins have been discovered to be involved in linking cell proliferation control and ribosome biogenesis in yeast (Srivastava and Pollard, 1999; Du and Stillman, 2002; Jorgensen et al., 2002; Zhang et al., 2002; Bernstein et al., 2007). Mutations in genes involved in RNA processing, including *SWA1* (Shi et al., 2005), *GFA1/CLO1*, and *ATROPOS* (*ATO*; Moll et al., 2008; Liu et al., 2009; Yagi et al., 2009), lead to slow progression of the division cycle during female gametogenesis. Intriguingly, mutation in *LACHESIS* (*LIS*), coding for a putative splicing factor, promotes egg cell fate in the synergid and the central cell at the expense of the synergid and central cell fate (Groß-Hardt et al., 2007), suggesting that *LIS* plays a pivotal role in suppressing the egg cell fate in the synergid and the central cell as well as the central cell fate in antipodal cells. Similarly, cell fate changes have also been observed in *gfa1/clo1* and *ato* mutants (Moll et al., 2008). These data imply that RNA processing and ribosome biogenesis play a key role in coordinating cell cycle progression and cell fate. Here, we report the genetic and molecular characterization of a *swa2* mutation that impairs cell growth and cell division in Arabidopsis. *SWA2* encodes a nucleolar protein homologous to yeast NUCLEOLAR COMPLEX ASSOCIATED PROTEIN1 (NOC1)/MAINTENANCE OF KILLER21 (MAK21) that is essential for ribosome biogenesis in yeast. We also show that SWA2 interacts physically with NOC2 homologues in yeast cells. Together, these data indicate that SWA2 is most likely involved in ribosome biogenesis and essential for cell cycle progression in female gametophyte development in Arabidopsis.

RESULTS

Isolation and Genetic Characterization of the *swa2* Mutant

To identify mutations affected in cell growth and division during female gametophyte development, a screen for distorted Mendelian segregation was carried out as described previously (Springer et al., 1995; Sundaresan et al., 1995; Pagnussat et al., 2005). One mutant, *swa2*, was isolated that exhibited an aberrant kanamycin resistant-to-kanamycin sensitive (Kan^R:Kan^S) segregation ratio of 1:1 (Kan^R:Kan^S = 661:663). Siliques from *swa2* heterozygous plants contained about 31.5% (n = 964 ovules) aborted ovules (Fig. 1), suggesting that it is likely defective in gametophytic function.

To analyze the transmission of *swa2* through female germ lines, we performed crosses between *swa2* and wild-type plants and traced the presence of *Ds* insertion in the F1 progeny. When the heterozygous mutant was used as the egg donor, the transmission efficiency to the mutation was 19% (n = 759), indicating that the mutation has a strong defect in female gametophytes. In addition, approximately 6% (n = 964) of selfed F1 seeds displayed embryo arrest before the globular stage, and no homozygous plants were obtained. This suggested that the mutant is homozygous lethal. Therefore, we use *swa2* to represent the heterozygous

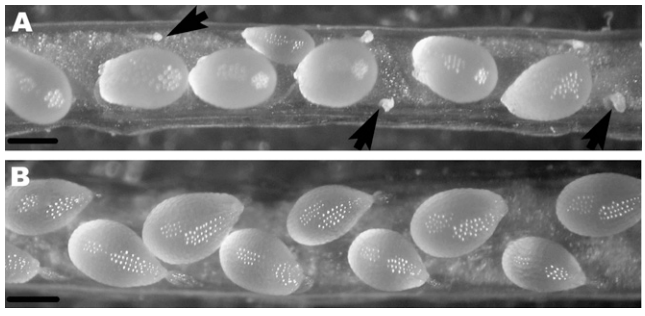

Figure 1. Phenotype of the *swa2* plant. A, A *swa2* silique showing aborted ovules (black arrows). B, A wild-type silique showing a full seed set. Bars = 100 μm.

mutant (*Ds*/+) in this paper. Overall, the mutant plants are morphologically normal except that they bear shorter siliques than the wild-type plants.

Synchrony of Female Gametophyte Development Is Impaired in *swa2*

To characterize the mutant phenotype, we examined ovule development in wild-type and *swa2* plants using confocal laser scanning microscopy. Female gametophyte (FG) development in Arabidopsis is divided into seven distinct stages (Christensen et al., 1997, 2002), as shown in Figure 2. The functional megaspore (FG1; Fig. 2A) undergoes mitosis to give rise to a two-nucleate embryo sac (FG2; Fig. 2B). A central vacuole is formed between the two nuclei and pushes them apart from each other (FG3; Fig. 2C). The two nuclei undergo a second division to give rise to a four-nucleate embryo sac at early FG4 (Fig. 2D). At this time, the division plane between the two chalazal nuclei lies parallel to the chalazal-micropylar axis. Then, two of the four nuclei migrate so that the division plane between them is orthogonal to the axis (Fig. 2E). Another round of division takes place

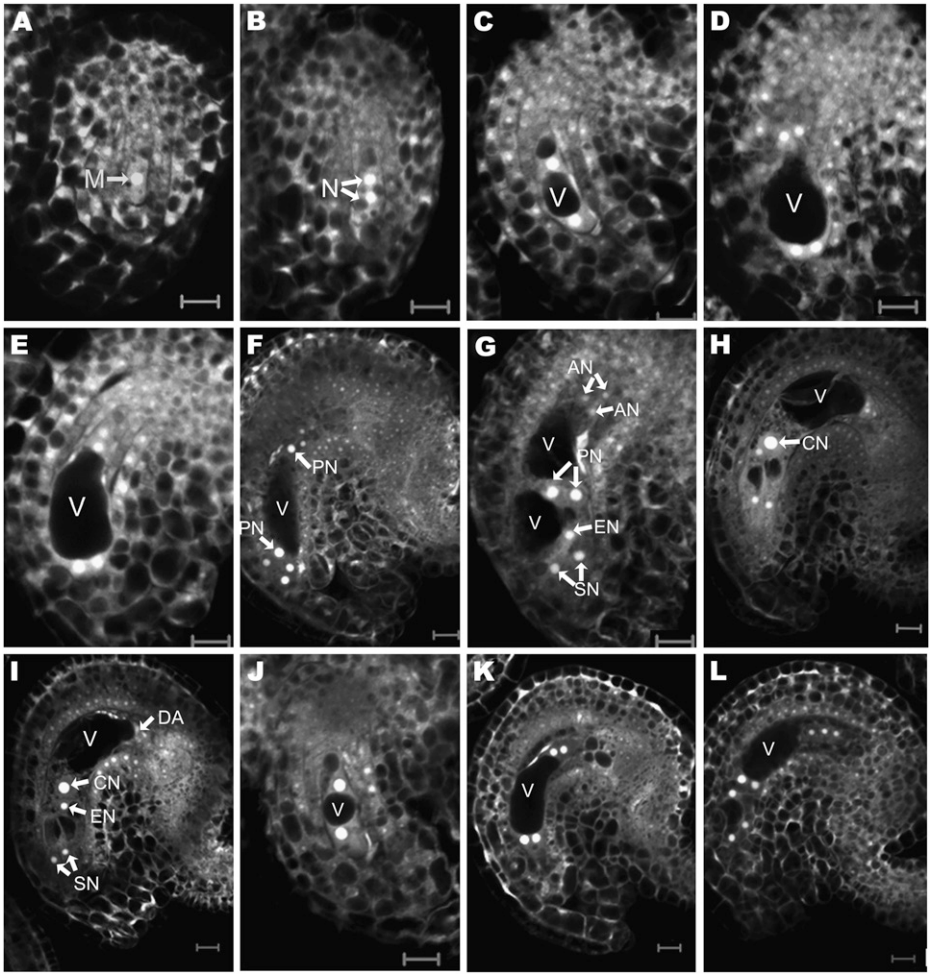

Figure 2. Ovule development revealed by confocal laser scanning microscopy in wild-type and *swa2* plants. A, An FG1-stage ovule showing the functional megaspore (M). B, An FG2-stage ovule with a two-nucleate (N) embryo sac. C, An FG3-stage ovule showing a late two-nucleate embryo sac with an enlarged central vacuole (V) and a small chalazal vacuole. D, An ovule at early FG4 stage. The line between the two chalazal nuclei lies parallel to the chalazal-micropylar axis. E, An ovule with a four-nucleate embryo sac at late FG4 stage. Note that the division planes of the chalazal and the micropylar nuclei are perpendicular to each other. F, An ovule at early FG5 stage with an eight-nucleate embryo sac in a 4n + 4n configuration. The polar nuclei (PN) are recognizable. G, An ovule image showing an embryo sac at FG5 stage. Cellularization took place and cell differentiation was completed with the formation of two synergic nuclei (SN), an egg nucleus (EN), three antipodal nuclei (AN), and the two prominent polar nuclei, which have not fused yet. H, An ovule with a mature seven-celled embryo sac at stage FG6. Note that the polar nuclei fused to form a diploid central nucleus (CN). I, An ovule at FG7 stage, in which the antipodal cell began to degenerate (DA). J, A micrograph showing a mutant ovule arrested at FG3. K, A micrograph showing a mutant ovule arrested at FG4. L, A micrograph showing a mutant ovule arrested at FG5. All images were projected from multiple 1-μm optical sections. The developmental stages are defined according to Christensen et al. (1998). Bars = 5 μm.

Table I. *Synchrony of female gametophyte development in wild-type Arabidopsis*

Pistil Number	Number of Female Gametophytes at Developmental Stages							
	FG1	FG2	FG3	FG4	FG5	FG6	FG7	Total Female Gametophytes
1	27	11	2					40
2	6	17	6	3				32
3	2	18	6					26
4		4	25	7				36
5			12	35	3			50
6			3	17	21			41
7			5	9	39	2		55
8				2	32	17		51
9					20	17	2	39
10					16	30	4	50
11					6	36	9	51
12						4	46	50

to give rise to an eight-nucleate embryo sac (FG5; Fig. 2F). The two polar nuclei, one from each pole, migrate toward the micropylar half of the developing female gametophyte (Fig. 2G) and eventually fuse to form the central cell (FG6; Fig. 2H). The three antipodal cells degenerate just before fertilization, and the mature female gametophyte consists of two synergid cells, one egg cell, and one central cell (FG7; Fig. 2I). In wild-type plants, ovule development in a pistil is synchronous with only a narrow range of variations (Christensen et al., 1997; Shi et al., 2005). At 24 h after emasculation, most ovules in a wild-type pistil were found in FG6 or FG7. However, in the mutant pistils, we found that about half of the ovules were at FG6 or FG7 representing the wild-type ovules and the other half were arrested at different stages, including FG3, FG4, and FG5 (Fig. 2, J–L). These data indicated that the cell cycle progression in the mutant female gametophyte was impaired.

To further investigate whether the synchronous development of female gametophytes in the mutant pistils was affected, we performed a detailed study of synchrony in wild-type and mutant ovules. Pistils from the same inflorescence were opened sequentially, and ovules from each pistil were dissected out and checked for their development stages. The numbers of ovules at each stage were counted. The results are summarized in Tables I and II. In the wild-type plant, most ovules within the same pistil are often at either one or two adjacent developmental stages (Table I). This observation is consistent with previous studies (Christensen et al., 1997; Shi et al., 2005), which indicate that embryo sac development within a pistil is synchronous to a large extent. However, in the mutant plants, the development of the embryo sacs is asynchronous, and ovules within the same pistil are arrested at several developmental stages (Table II). These data suggested that the progression of the gametophytic nuclear division was retarded in the mutant embryo sacs.

To investigate whether the retarded female gametophyte in the mutant ovule is able to form a functional embryo sac, we performed a delayed pollination test according to Shi et al. (2005). Pistils of *swa2* plants were emasculated at floral stage 12c (Smyth et al., 1990) and pollinated with pollen from wild-type plants at 12, 24, 36, 48, or 72 h after emasculation. F1 seeds from three independent plants of each group were collected and

Table II. *Synchrony of female gametophyte development in swa2 plants*

Pistil Number	Number of Female Gametophytes at Developmental Stages							
	FG1	FG2	FG3	FG4	FG5	FG6	FG7	Total Female Gametophytes
1	31	6	7					44
2	29	4	6					39
3	16	11	13	3				43
4	2	8	9	15	2			36
5	4	11	9	4	11	1		40
6	1	1	20	13	18			53
7		2	15	5	18	3		43
8			6	13	10	12		41
9			1	32	14	15		62
10			2	18	6	23	2	51
11			1	8	15	1	21	46

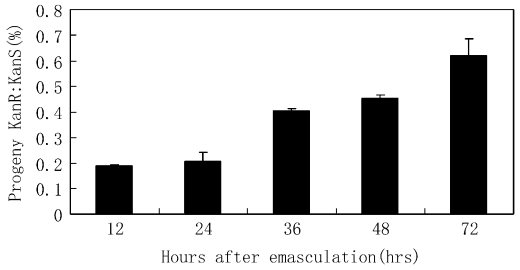

Figure 3. Segregation ratio of F1 progeny from the delayed pollination test. The *swa2* plants were emasculated at floral stage 12c (Smyth et al., 1990) and pollinated with pollen from wild-type plants at 12, 24, 36, 48, or 72 h after emasculation. Kan^R:Kan^S ratios of the F1 progeny of each group were analyzed.

examined for Kan^R:Kan^S ratio. As the pollination was postponed, the Kan^R:Kan^S ratio of the F1 progeny increased from 18.8% when pollinated at 12 h after emasculation to 60.7% when pollinated at 72 h after emasculation (Fig. 3), indicating that more mutant ovules were fertilized and produced seeds. These results suggested that although the mutant ovules develop more slowly than their wild-type counterpart, they have the potential to develop into functional female gametophytes and could be fertilized.

In conclusion, the *swa2* mutant displayed retarded progression of the gametophytic division cycles and asynchronous development of the female gametophyte. The mutant embryo sacs reach the mature stage and could be fertilized by delayed pollination.

Pollen Development Is Defective in the *swa2* Mutant

To analyze whether the mutation also affected the male germ line, we performed crosses between wild-type and *swa2* plants and traced the presence of the *Ds* insertion in the F1 progeny. When the heterozygous mutant was used as the pollen donor, the transmission efficiency was 82% (n = 1,374), indicating that the mutation has a slight effect in male gametophytes.

To further clarify the defect in pollen, 4′,6-diamino-2-phenylindole (DAPI) staining was performed to check male gametophytic cell cycle progression. At anthesis, wild-type pollen completed mitosis II and displayed a typical tricellular configuration, in which the vegetative cytoplasm contains one vegetative nucleus and two highly condensed sperm nuclei (Fig. 4A). Wild-type plants showed less than 1% aberrant pollen with disrupted positioning or aberrant appearance of the nuclei. In the mutant, about 9.4% (n = 832) of pollen showed an abnormal cell cycle, with 5.3% of pollen grains arrested at the bicellular stage (Fig. 4B) and 4.1% of mutant pollen completing pollen mitosis II, but the sperm nuclei were less condensed and appeared thread shaped (Fig. 4, B and C). These data indicated that the mutation also affects the cell cycle in pollen, mainly causing the slowing of pollen mitosis, although to a lesser extent compared with that in female gametophytes.

SWA2 Encodes a NOC1 Homologue

Thermal asymmetric interlaced PCR (Liu et al., 1995; Grossniklaus et al., 1998) was used to isolate the genomic sequences flanking the *Ds* element. Sequence analysis revealed that the *Ds* was inserted at 27 bp upstream the ATG of *At1g72440* (Fig. 5A). Southern-blot analysis showed that a single *Ds* element was inserted in the genome of *swa2* (data not shown). To confirm whether the mutant phenotype of *swa2* was indeed caused by the *Ds* insertion of *At1g72440*, a 9,024-bp genomic fragment from −827 bp upstream of the start codon to 2,928 bp downstream of the stop codon of *At1g72440* was cloned to pCAMBIA1301 and introduced into the heterozygous *swa2* plants. Twenty-nine transgenic lines were obtained by kanamycin and hygromycin double selection. Seed set of these T1 plants was restored to 76% to 90% in independent lines, compared with 62.5% in *swa2* plants. Ten independent lines were randomly chosen for further statistical analysis. Progeny of these lines showed a Kan^R:Kan^S ratio of 1.77 to 2.85, compared with 1.0

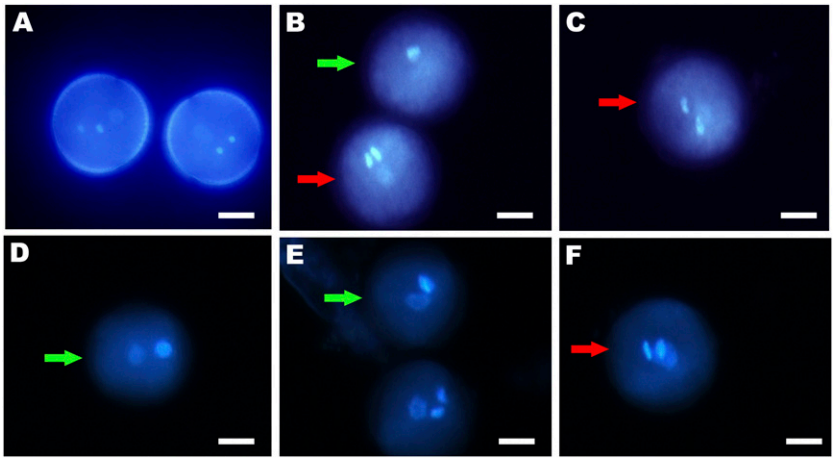

Figure 4. The pollen showed defective cell cycle progression in the *swa2* mutant. A, A micrograph showing wild-type pollen grains at maturity. Note the condensed sperm nuclei. B, A micrograph showing *swa2* pollen grains arrested at either the bicellular stage (green arrow) or the tricellular stage with sperm nuclei defective in chromosome condensing (red arrow). C, A micrograph showing a mutant pollen grain with thread-like sperm nuclei (red arrow). D, A micrograph showing a pollen grain of *salk_016552* arrested at the bicellular stage (green arrow). E, A micrograph showing pollen grains of *salk_016552* arrested at the bicellular stage (green arrow) compared with the wild-type pollen grain. F, A micrograph showing thread-like nuclei of a pollen grain of *salk_016552* (red arrow). Bars = 10 μm.

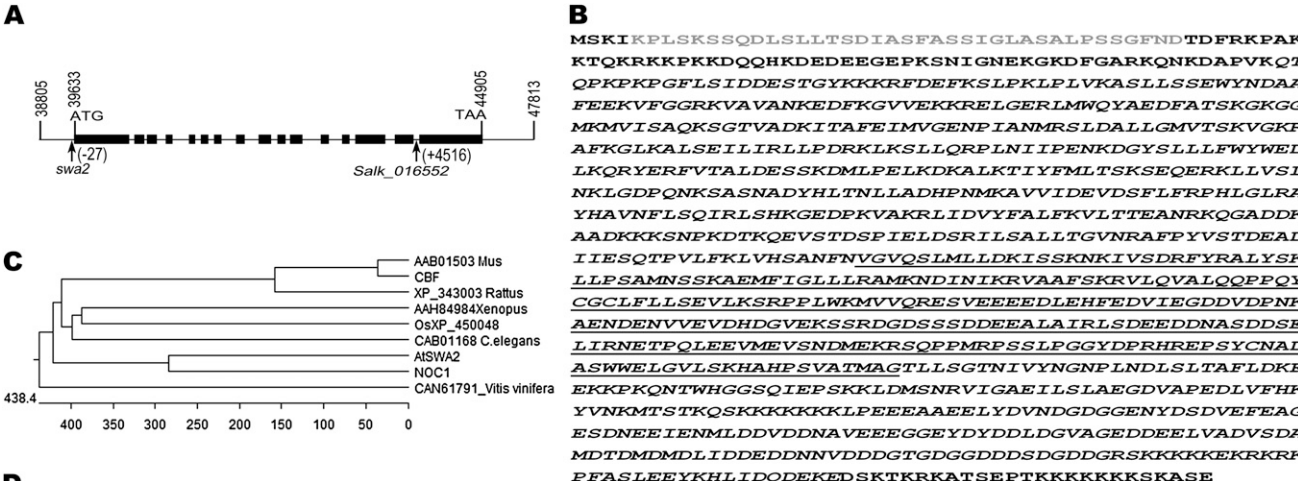

Figure 5. Molecular characterization of *SWA2*. A, Diagram of the insertion positions of *Ds* (*swa2*) and *T-DNA* (*Salk_016552*) in *SWA2*. The black boxes indicate the exons of the *SWA2* gene. The shaded amino acids at the N terminus show the N-terminal JmjN domain found in the Jumonji transcription factor. The nucleotide numbers are consistent with those in bacterial artificial chromosome clone T10D10. B, Predicted SWA2 amino acid sequence. The italic amino acids represent the putative nucleic

in the mutant. Furthermore, we obtained several T3 plants that were completely resistant to kanamycin and hygromycin. Siliques of these plants showed full seed set, indicative of complete complementation. These data confirmed that the mutant phenotype was indeed caused by the loss of function of *At1g72440*.

We then searched for additional T-DNA insertion lines in the *At1g72440* gene. A T-DNA insertion line, *salk_016552*, was identified in which the T-DNA was inserted into the last intron of *At1g72440* (Fig. 5A). This mutant displayed 43.5% (n = 989) seed abortion and about 8% defective pollen with abnormal nuclei (Fig. 4, D–F). Morphologically, the embryo sac phenotype of *salk_016552* is the same as that of the *Ds* insertion line (data not shown). These data together with the complementation results demonstrated that *At1g72440* corresponds to the *SWA2* gene.

To determine the gene structure of *At1g72440*, cDNA was isolated by reverse transcription (RT)-PCR from Arabidopsis ecotypes Landsberg *erecta* and Columbia. Sequencing results revealed that the second exon was 39 bp shorter compared with the predicted cDNA sequence of *At1g72440* at The Arabidopsis Information Resource database (http://www.arabidopsis.org). Thus, the *SWA2* gene encodes a putative protein of 1,043 amino acids (Fig. 5B). Sequence analysis with BLAST and SMART revealed that SWA2 contains an N-terminal JmjN domain found in the Jumonji transcription factor family, a central nucleic acid-binding domain (resides 97–1,018) possibly involved in ribosome biogenesis, and a C-terminal nuclear localization signal (residues 1,023–1,040; Fig. 5B). Within the nucleic acid-binding domain, there are several motifs such as CCAAT-BOX BINDING FACTOR (CBF; residues 520–772) and TOPEUc (DNA Topoisomerase I in eukaryota; residues 130–335) that are present in the C terminus of eukaryotic DNA topoisomerase, DEXDc, found in DEAD and DEAH box helicases involved in RNA metabolism, and divergent HEAT repeats involved in ribosome synthesis and export (Dlakic and Tollervey, 2004). BLAST analysis indicated that *SWA2* is a single-copy gene in Arabidopsis, and the SWA2 protein shares high homology with proteins from many eukaryotic species. Phylogenetic analysis showed that the yeast NOC1 (MAK21) protein is most similar to SWA2 (Fig. 5C). They share 31% identity and 53% similarity at the amino acid level (Fig. 5D). In yeast, NOC1 (MAK21) is a nucleolar protein involved in nuclear export of preribosomes (Edskes et al., 1998; Milkereit et al., 2001).

SWA2 Protein Is Localized in the Nucleolus

To determine the subcellular localization of SWA2, a C-terminal translational fusion of *SWA2* with *DsRed2* driven by the *SWA2* native promoter was cloned into pCAMBIA1300 and introduced into *swa2* plants. Transgenic plants selected by hygromycin and kanamycin double selection showed rescued Kan^R:Kan^S segregation ratio and seed set (data not shown), indicating that the fusion protein functionally complemented the mutant phenotype. Confocal laser scanning microscopy revealed that the fusion protein was localized in the nucleolus of root cells at interphase (Fig. 6). These results demonstrated that SWA2 is a nucleolar protein, consistent with its putative role in preribosome transport.

SWA2 Interacts with the NOC2 Homologue in Yeast

Since SWA2 is homologous to NOC1 and localized to the nucleolus, it might be involved in nucleolar function such as ribosome biogenesis. In *Saccharomyces cerevisiae*, NOC1/MAK21 interacts with NOC2 and is required for ribosome maturation and transport (Milkereit et al., 2001). There are two NOC2 homologues in Arabidopsis, *At2g18220* and *At3g55510*, and the former is more similar to NOC2. To investigate whether *SWA2* plays a similar role as NOC1, we tested whether SWA2 interacts with Arabidopsis NOC2 homologues using a yeast two-hybrid assay. A full-length *SWA2* coding sequence was constructed into pGBKT7, and truncated *At2g18220* cDNA and full length *At3g55510* cDNA were constructed into pGADGH. Yeast cells contransformed with pAD-At2g18220 and pBD-SWA2 grew well in Trp-, Leu-, and His-dropout medium supplemented with 10 mM 3-amino-1,2,4-triazole (3-AT). However, cells transformed with pAD-At3g55510 and pBD-SWA2 did not grow (Fig. 7A). These data suggested that SWA2 physically interacts with At2g18220 but not with At3g55510 in yeast cells. Expression pattern analysis using available microarray data sets (https://www.genevestigator.ethz.ch; Zimmermann et al., 2004) showed high correlation of the expression profiles between *SWA2* and *At2g18220* (Fig. 7B), which suggests that the two proteins may interact with each other in planta.

Expression Pattern of the *SWA2* Gene

To investigate the expression pattern of the *SWA2* gene in different organs, RT-PCR was performed with total RNA from roots, stems, leaves, inflorescences, siliques, and seedlings. A single band with the expected

Figure 5. (*Continued.*)
acid-binding domain possibly involved in ribosomal biogenesis, and the divergent HEAT repeats are underlined, which overlap the conserved CBF domain. The underlined amino acids at the C terminus show the predicted nuclear localization signal. C, Phylogenetic tree of SWA2 with its homologues from other organisms. D, Alignment of the SWA2 protein with its homologues from rice (*Oryza sativa* 'Japonica'), yeast, human, and mouse. Identical amino acids are shown with gray letters in black boxes, and similar amino acids are shown with shaded boxes.

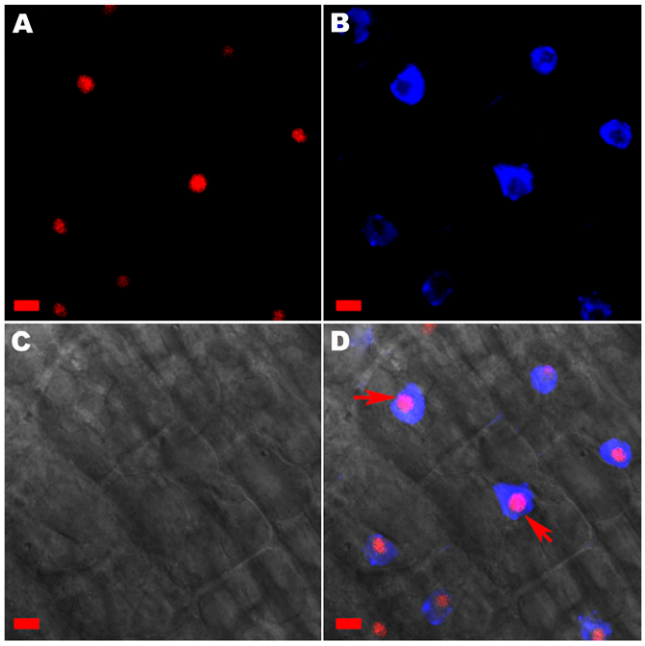

Figure 6. Subcellular localization of the SWA2-DsRed2 fusion protein in Arabidopsis root cells. A, Confocal image of a transgenic root cell under the DsRed2 channel showing SWA2-DsRed2 localization (red). B, The same image as in A showing DNA visualized with DAPI staining (blue). C, The same image as in A under bright-field illumination. D, Merged image of A, B, and C showing the nucleolar localization of SWA2-DsRed2. The arrows show the signal of SWA2-DsRed2 (red) and DNA (blue). Bars = 5 μm.

size was detected in RNAs from all tissues, with the highest expression level in inflorescences, seedlings, and leaves (Fig. 8A). These data are consistent with the microarray data available at Genevestigator (Fig. 8B; https://www.genevestigator.ethz.ch).

To further study the expression pattern of *SWA2*, a P_{SWA2}:*SWA2*:*GUS* reporter system was used to monitor its expression. The full-length 9,024-bp genomic sequence of *SWA2* was fused in-frame with the *GUS* reporter gene and subcloned into pCAMBIA1300. The construct was introduced into Arabidopsis Landsberg *erecta* plants. In T2 transgenic plants, GUS activity was detected in the nucleolus in actively dividing tissues, such as root tips, lateral root primordia, shoot apices, young leaves, inflorescences, and pollen grains (Fig. 8, C–E). During female gametophyte development, strong GUS activity was detected in the gametophytic nucleus from one-nucleate to two-nucleate stages (Fig. 8, F and G). At the four-nucleate stage (FG4), the GUS activity became much weaker (data not shown). In the mature embryo sac just before fertilization, only the central cell showed strong GUS staining (Fig. 8H), indicating that *SWA2* is expressed differentially in the mature embryo sac.

DISCUSSION

The coordination of cell growth, division, and differentiation is fundamental to development in multicellular organisms. However, mechanisms that couple growth and division, for example, have been investigated mainly in single-cell organisms or cultured cells. The developmental process of the haploid female gametophyte in Arabidopsis provides an excellent system to address how cell growth and division are coupled as well as the biological significance of such coupling to development (Grossniklaus and Schneitz, 1998; Yang and Sundaresan, 2000). We and others have previously isolated mutations that disrupted the pro-

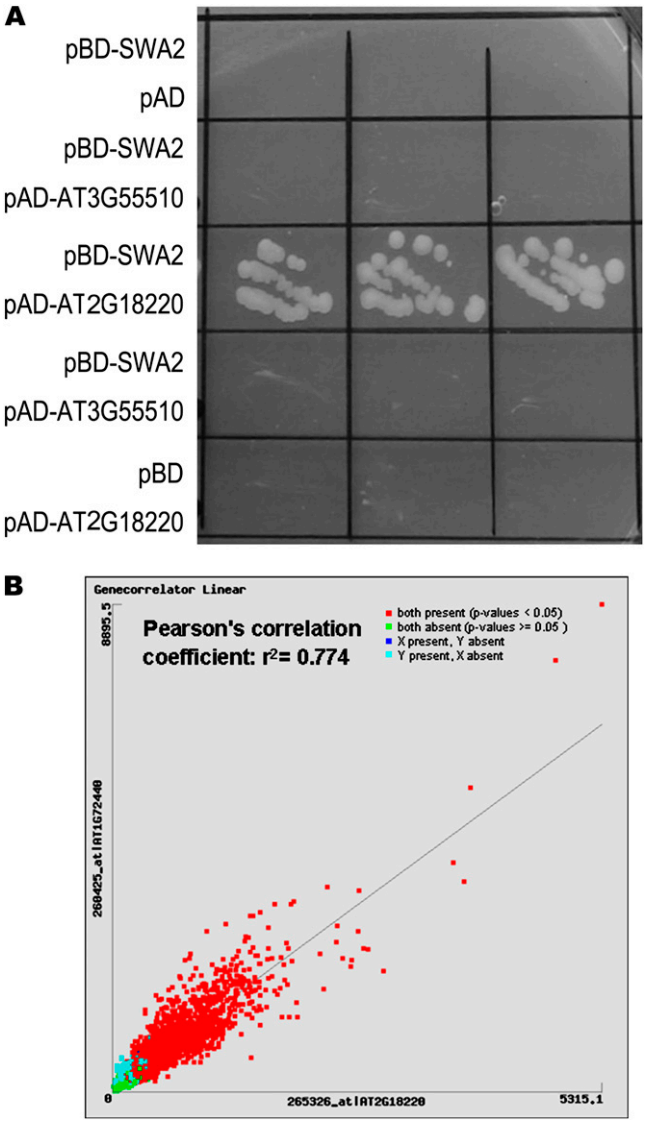

Figure 7. SWA2 interacts with the Arabidopsis NOC2 homologue in yeast cells. A, SWA2 interacts with At2g18220 but not At3g55510 in yeast cells. For each transformation, three independent transformants were streaked on a plate containing synthetic dropout selection medium that lacked Trp, Leu, and His supplemented with 10 mM 3-AT. B, Correlation of the expression profiles of *SWA2* and *At2g18220*. Data were retrieved from the public Genevestigator microarray data set (https://www.genevestigator.ethz.ch; Zimmermann et al., 2004). [See online article for color version of this figure.]

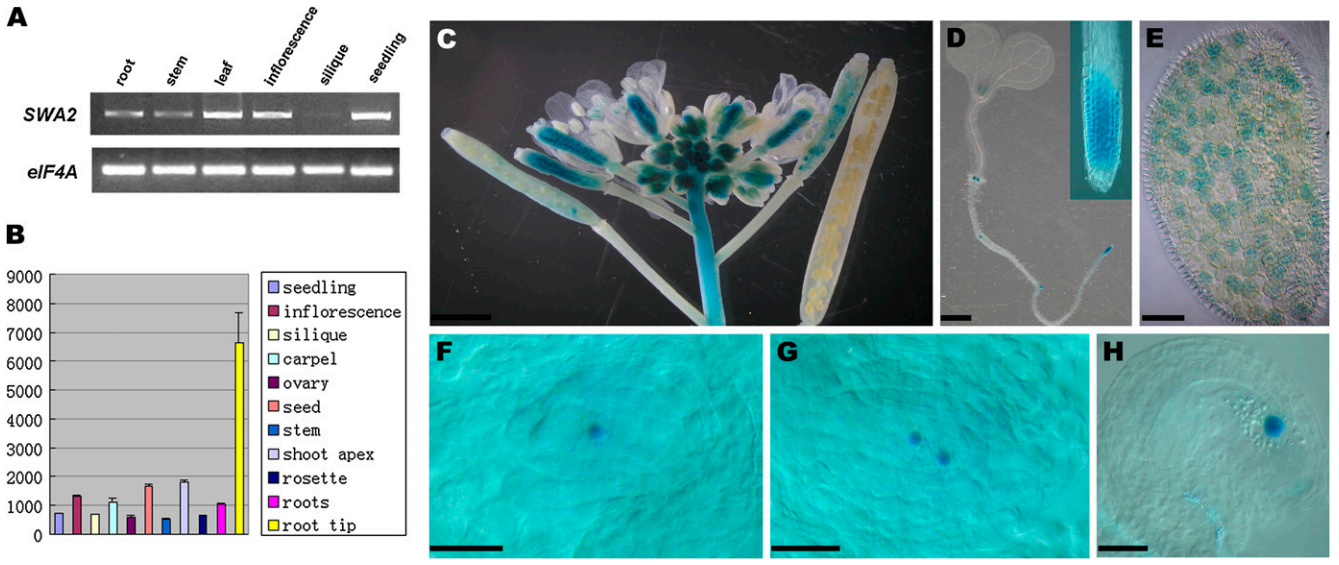

Figure 8. Expression pattern of the *SWA2* gene as revealed by RT-PCR analysis (A), RNA profiling (B), and transgenic plants expressing P_{SWA2}:*SWA2*:*GUS* reporter (C–H). A, Tissue-specific expression of *SWA2* using RT-PCR analysis. RT-PCR was performed on total RNAs from different tissues, including roots, stems, leaves, inflorescences, siliques, and seedlings as indicated. After 32 cycles, the resulting products were stained with ethidium bromide and analyzed by gel electrophoresis. *EIF4A* RNA was used as an internal template control. B, Expression profiles of *SWA2* in various organs. The *y* axis represents the expression level. Data used in this analysis were retrieved from the public Genevestigator microarray data set (https://www.genevestigator.ethz.ch; Zimmermann et al., 2004). C, A micrograph showing GUS activity specifically detected in floral meristem and young siliques of P_{SWA2}:*SWA2*:*GUS* transgenic Arabidopsis. Bar = 1 mm. D, A micrograph showing GUS activity in the shoot apex, leaf primordium, lateral root primordia, and root meristem in a 7-d-old P_{SWA2}:*SWA2*:*GUS* transgenic seedling. Bar = 1 mm. E, A micrograph showing GUS activity in pollen grains. Bar = 10 μm. F, A micrograph showing GUS activity in a one-nucleate embryo sac. Bar = 5 μm. G, A micrograph showing GUS activity in an early two-nucleate embryo sac. Bar = 5 μm. H, A micrograph showing GUS activity in the central cell nucleus of a mature embryo sac. Bar = 5 μm.

gression of the mitotic division cycle during female gametogenesis in Arabidopsis (Moore et al., 1997; Christensen et al., 1998; Shi et al., 2005). The characterization of these mutations is starting to shed light on how cell growth, division, and cell fate are coupled (Shi et al., 2005; Groß-Hardt et al., 2007; Moll et al., 2008; Liu et al., 2009; Yagi et al., 2009).

SWA2 Is Most Likely Involved in Ribosome Biogenesis in Plants

SWA2 encodes a nucleolar protein that shows high homology to yeast NOC1/MAK21. In yeast, it was reported that NOC1 interacts with NOC2 and is involved in preribosome biogenesis and nucleolar export (Edskes et al., 1998; Milkereit et al., 2001). NOC1 is a conserved protein during evolution, and there is only one homologue in almost all eukaryotes, so it is likely that its function in ribosome biogenesis is also conserved. The high homology with NOC1, its nucleolar localization, and interaction with an Arabidopsis NOC2 homologue all suggest that SWA2 is most likely involved in ribosome biogenesis in plants. However, in our experiments, *SWA2* failed to functionally complement a yeast *noc1/mak21* mutant (data not shown). This might be due to divergence of the protein structure of the NOC1 and/or NOC2 component of the ribosome-exporting complex, although it is functionally conserved during evolution. It was reported that the human homologue of NOC, CBF, could not functionally complement the yeast *noc1* mutation (Edskes et al., 1998). This suggested that the human CBF and the yeast NOC1 are either functionally different or have diverged in structure.

Previously, we identified a group of female gametophytic mutants that displayed delayed progression of the division cycle and designated them *swa* mutations. *swa2*, also named *embryo sac development arrest25* (*eda25*) in the large-scale screen for female gametophytic mutations (Pagnussat et al., 2005), is phenotypically similar to *swa1* (Shi et al., 2005). Both *swa1* and *swa2* mutations disrupted the progression of the female gametophytic division cycle and showed a retarded development phenotype. Like *SWA2*, *SWA1* also encodes a nucleolar protein with a WD40 domain that is involved in 18S pre-rRNA processing in Arabidopsis (Shi et al., 2005). These findings suggest that they may act in the same pathway to modulate ribosome biogenesis during female gametophyte development.

Nucleolar Function Is Essential for Progression of the Division Cycle during Female Gametogenesis in Plants

The nucleolus may not be just the site of rDNA transcription and ribosome biogenesis, as in our con-

ventional perception (Raška et al., 2004, Boisvert et al., 2007). More and more studies have shown that the nucleolus is also involved in controlling mitosis, cell cycle progression, and cell proliferation (Cockell and Gasser, 1999; Carmo-Fonseca, 2002; Shaw and Doonan, 2005). Nucleolar proteomics data showed that the nucleolus contains proteins related to these functions (Leung et al., 2003; Coute et al., 2006). In yeast, nucleolar proteins were found functioning in the coordination of cell proliferation, DNA replication, and ribosome biogenesis (Wade et al., 2001; Du and Stillman, 2002; Zhang et al., 2002). Mutations of these nucleolar proteins cause delayed or arrested cell cycle progression. Consistently in plants, several mutations in genes coding for nucleolar proteins, such as *SWA1* (Shi et al., 2005), *TORMOZ* (Griffith et al., 2007), *DOMINO1* (Lahmy et al., 2004), *LIS* (Groß-Hardt et al., 2007), and *GFA1/CLO* and *ATO* (Moll et al., 2008; Liu et al., 2009; Yagi et al., 2009), causing defects in ribosome biogenesis or nucleolar function, have been shown to affect cell proliferation during female gametophyte and embryo development. More intriguingly, gametic cell fates are altered in *lis* (Groß-Hardt et al., 2007) and *gfa1/clo/ato* (Moll et al., 2008) mutants. These data suggest a key role of nucleolar function in female gametophyte development in plants.

Ribosome biogenesis and dynamics are central for cell growth, and it was estimated that yeast cells must synthesize more than 2,000 ribosomes and transport about 1,000 ribosomal proteins from cytoplasm to the nucleolus per minute (Warner et al., 2001). Therefore, the coordination of rRNA transcription with ribosomal protein synthesis and transportation must be tightly regulated. More importantly, ribosome biogenesis must be coordinated with cell state, cell division, and development. Elucidation of genetic mechanisms governing these processes will shed light on the understanding of how cells sense intrinsic cellular activities in a developmental context.

MATERIALS AND METHODS

Plant Material and Growth Conditions

The *swa2* mutant of Arabidopsis (*Arabidopsis thaliana*) was isolated from a genetic screen of *Ds* insertion lines as described previously (Sundaresan et al., 1995; Shi et al., 2005). Seeds were sterilized with 20% bleach for 5 to 10 min, then washed five times in sterilized water and germinated on Murashige and Skoog agar plates. For antibiotic selection, 50 mg L^{-1} kanamycin and/or 20 mg L^{-1} hygromycin were supplemented as required. Seeds were stratified in darkness at 4°C for 3 d before growing in growth chambers at 22°C ± 2°C under a 16-h-light/8-h-dark cycle. Plant transformation was performed by *Agrobacterium tumefaciens*-mediated infiltration (Bechtold and Pelletier, 1998).

Phenotypic Analysis by Confocal Laser Scanning Microscopy

Confocal observation of ovules was performed as described previously (Christensen et al., 1998; Shi et al., 2005). Inflorescences were fixed in 4% glutaraldehyde in 12.5 mM cacodylate (pH 6.9) overnight at room temperature. The tissue was then dehydrated through a conventional ethanol series with 30 min per step. The dehydrated tissue was cleared in 2:1 (v/v) benzyl benzoate: benzyl alcohol for 1 h. Pistils were dissected, mounted with immersion oil, and observed using a Zeiss LSM510 META laser scanning microscope with a 488-nm argon laser and an long-pass 530 filter.

Reciprocal Crosses and Delayed Pollination Test

Reciprocal crosses between wild-type and *swa2* plants were performed as described (Yang et al., 1999). The delayed pollination test was performed according to Shi et al. (2005) with slight modifications. Anthers of *swa2* plants were removed at stage 12c (Smyth et al., 1990) and pollinated with wild-type pollen at 12, 24, 36, 48, or 72 h after emasculation. The F1 seedlings were scored for kanamycin resistance on Murashige and Skoog plates according to Sundaresan et al. (1995).

Pollen Analysis

For light and fluorescence microscopy of pollen, specimens were observed using a Zeiss Axioskop II microscope, and images were acquired with a Cannon PowerShot G6. Staining assay with DAPI was performed as described previously (Johnson-Brousseau and McCormick, 2004), and DAPI concentration was at 1 μg mL^{-1}.

Molecular Cloning and Genetic Complementation

The *Ds* flanking sequences were isolated by thermal asymmetric interlaced PCR as described (Liu et al., 1995; Yang et al., 1999). For the complementation construct, two genome fragments were amplified by KOD+ polymerase (Toyobo) using primers P290CPF-KPN (5′-GGGGTACCCCTCCAAAACCAAAGGCCCATAACC-3′) and P290G-M-SAL-PST (5′-GTCGACATCGAAAATTTAATAACAAAAGAA-3′) for fragment 290CPa and P290CPRV-PST (5′-AACTGCAGCTTCTGAGAGTTCGTCGGAAACAGC-3′) and P290G-M-SAL-KPN (5′-GTCGACACACTGTATAGTAAATTTTTTTGT-3′) for 290CPb. The two fragments were first cloned into pGEM-T Easy (Promega) and then subcloned into pCAMBIA1301 (www.cambia.org.au) at *Kpn*I/*Sal*I and *Sal*I/*Pst*I sites, respectively, to produce p1301-290CP containing the full-length genomic fragment form from −827 bp upstream of the ATG start codon to 2,928 bp downstream of the stop codon of *At1g72440*. The construct was introduced into *swa2* plants by *Agrobacterium*-mediated infiltration (Bechtold and Pelletier, 1998).

The SWA2-DsRed2 Construct and Subcellular Localization

The *DsRed2* coding sequence was amplified from pDsRed2 (Clontech) using primers PDsRed2F-KPN (5′-GGGGTACCATGGCCTCCTCCGAGAACGTCA-3′) and PDsRed2-RV-SAC (5′-GGGGAAGCTTGAGCTCTACAGGAACAGGTGGTGGCGGC-3′) and inserted into pCAMBIA1300 at the *Kpn*I and *Sac*I sites. The 2,928-bp fragment downstream of the stop codon of *SWA2* was amplified using primers P2903UTR+Sstup (5′-GGAGAGCTCGAAGCAAGACTTGTTGCTTG-3′) and P290CPRV-ECOR (5′-GGAATTCCTTCTGAGAGTTCGTCGGAAACAGC-3′) and inserted into the construct pCAMBIA1300-DsRed2 at *Sac*I and *Eco*RI sites. The 6,093-bp promoter and coding region of *SWA2* was amplified using primers P290CPF-KPN (5′-GGGGTACCCCTCCAAAACCAAAGGCCCATAACC-3′) and P290STOPRV-KPN (5′-GGGGTACCCTCTGATGCTTTAGACTTCTTCTTT-3′) and inserted into the above construct at the *Kpn*I site to produce pCAMBIA1300-P_{swa2}:SWA2:DsRed2. Root tips of transgenic plants were stained with DAPI as described previously (Shi et al., 2005) and observed with the LSM510 META confocal microscope (Zeiss).

Yeast Two-Hybrid Assay

The full-length coding sequence of *SWA2* was amplified by PCR using the primers P290C-BD-NCO-F (5′-GGACCATGGACATGTCAAAGATAAAGCCTTT-3′) and P290C-PWM101-PSTDOWN (5′-GGACTGCAGTTACTCTGATGCTTTAGACT-3′) and cloned into pGBKT7 (Clontech) at *Nco*I and *Pst*I sites to give rise to pBD-SWA2. The cDNA fragment of *At2g18220* and the full-length coding sequence of *At3g55510* were amplified using primer P820ADF4-NDE (5′-GGAATTCCATATGAAGCGTGGGAAGAAGGTGAAATCTAA-3′) in combination with P820ADR4-XHO (5′-CCGCTCGAGAAGCTACTCGG-

GCCTTCTTCTTCTT-3′) and P510ADF-NDE (5′-GGAATTCCATATGGGT-AAGCTGGGGAAGAAAGCTA-3′) in combination with P510ADRV-XHO (5′-CCGCTCGAGTCACTTCTTCTTCTTGTTTGTTC-3′), respectively. The fragments were cloned into pGADGH at *Nde*I and *Xho*I sites. Yeast transformation was performed as described previously (Xie et al., 1999). The transformed cells were transferred to −Leu/−Trp/−His dropout supplement (BD Biosciences) plates supplemented with 1 to 10 mM 3-AT.

RNA Isolation and RT-PCR Analysis

Total RNA was isolated using TRIzol reagent (Invitrogen) and digested with RNase-free DNase I (Takara). One microgram of total RNA was used as a template to transcribe single-stranded cDNA by AMV reverse transcriptase (Takara). Mock controls without reverse transcriptase were performed simultaneously to detect genomic DNA contamination. One microliter of the synthesized cDNA and control products was used for PCR. Primers P290RTF1 (5′-CTCTGAATGGTACAACGATG-3′) and P290RTR1 (5′-CAGC-CTCGTCAGTGGAAACA-3′) were used for detection of *SWA2* expression, and primers PEIF4AF (5′-ATGGCAGGACCGCACCGGA-3′) and PEIF4ARV (5′-GCATGTCAAAAACACGACCGGGAGTTCC-3′) were used for amplification of the *EIF4A* gene as an internal control. PCR products were analyzed on 1% agarose gel.

Expression Analysis Using the GUS Reporter System

The *GUS* coding sequence was amplified from pWM101 (Ding et al., 2006) using primers PGUSF-KPN (5′-GGGGTACCATGTTACGTCCTGTAGAAAC-3′) and PGUSRV-PST (5′-AACTGCAGTCATTGTTTGCCTCCCTGCT-3′) and inserted into pCAMBIA1300 at the *Kpn*I and *Pst*I sites to produce pCAMBIA1300-GUS. The 6,093-bp fragment containing the promoter plus coding region and the fragment containing the 2,928-bp sequence downstream of the *SWA2* stop codon were amplified with primer pairs P290CPF-KPN (5′-GGG-GTACCCCTCCAAAACCAAAGGCCCATAACC-3′)/P290STOPRV-KPN (5′-GGGGTACCCTCTGATGCTTTAGACTTCTTCTTT-3′) and P2903UTR-F-PST (5′-AACTGCAGGAAGCAAGACTTGTTGCTTGCTATG-3′)/P290-STOPRV-KPN-GUS (5′-GGGGTACCCTCTGATGCTTTAGACTTCTTCTTT-3′), respectively. The resulting products were cloned into pCAMBIA1300-GUS at *Kpn*I and *Pst*I sites in the correct directions to produce the P_{SWA2}:SWA2:GUS construct. GUS activity assay of transgenic plants was performed as described previously (Ding et al., 2006).

Sequence data from this article can be found in the GenBank/EMBL data libraries under accession number EU170440.

ACKNOWLEDGMENTS

We thank Dr. Yan Guo and Dr. Feiyi Zhao at the National Institute of Biological Science, Beijing, for technical assistance in confocal microscopy.

Received June 6, 2009; accepted August 30, 2009; published September 4, 2009.

LITERATURE CITED

Bechtold N, Pelletier G (1998) In planta Agrobacterium-mediated transformation of adult *Arabidopsis thaliana* plants by vacuum infiltration. Methods Mol Biol **82:** 259–266

Bemer M, Wolters-Arts M, Grossniklaus U, Angenent GC (2008) The MADS domain protein DIANA acts together with AGAMOUS-LIKE80 to specify the central cell in *Arabidopsis* ovules. Plant Cell **20:** 2088–2101

Bernstein KA, Bleichert F, Bean JM, Cross FR, Baserga SJ (2007) Ribosome biogenesis is sensed at the Start cell cycle checkpoint. Mol Biol Cell **18:** 953–964

Boisvert FM, van Koningsbruggen S, Navascués J, Lamond AI (2007) The multifunctional nucleolus. Nat Rev Mol Cell Biol **8:** 574–585

Carmo-Fonseca M (2002) The contribution of nuclear compartmentalization to gene regulation. Cell **108:** 513–521

Christensen CA, Gorsich SW, Brown RH, Jones LG, Brown J, Shaw JM, Drews GN (2002) Mitochondrial GFA2 is required for synergid cell death in *Arabidopsis*. Plant Cell **14:** 2215–2232

Christensen CA, King EJ, Jordan JR, Drews GN (1997) Megagametogenesis in *Arabidopsis* wild type and the *Gf* mutant. Sex Plant Reprod **10:** 49–64

Christensen CA, Subramanian S, Drews GN (1998) Identification of gametophytic mutations affecting female gametophyte development in *Arabidopsis*. Dev Biol **202:** 136–151

Cockell M, Gasser SM (1999) Nuclear compartments and gene regulation. Curr Opin Genet Dev **9:** 199–205

Coute Y, Burgess JA, Diaz JJ, Chichester C, Lisacek F, Greco A, Sanchez JC (2006) Deciphering the human nucleolar proteome. Mass Spectrom Rev **25:** 215–234

Ding YH, Liu NY, Tang ZS, Liu J, Yang WC (2006) *Arabidopsis* GLUTAMINE-RICH PROTEIN23 is essential for early embryogenesis and encodes a novel nuclear PPR motif protein that interacts with RNA polymerase II subunit III. Plant Cell **18:** 815–830

Dlakic M, Tollervey D (2004) The Noc proteins involved in ribosome synthesis and export contain divergent HEAT repeats. RNA **10:** 351–354

Dow DA, Mascarenhas JP (1991) Synthesis and accumulation of ribosomes in individual cells of the female gametophyte of maize during its development. Sex Plant Reprod **4:** 250–253

Drews GN, Lee D, Christensen CA (1998) Genetic analysis of female gametophyte development and function. Plant Cell **10:** 5–17

Du YC, Stillman B (2002) Yph1p, an ORC-interacting protein: potential links between cell proliferation control, DNA replication, and ribosome biogenesis. Cell **109:** 835–848

Ebel C, Mariconti L, Gruissem W (2004) Plant retinoblastoma homologues control nuclear proliferation in the female gametophyte. Nature **429:** 776–780

Edskes HK, Ohtake Y, Wickner RB (1998) Mak21p of *Saccharomyces cerevisiae*, a homolog of human CAATT-binding protein, is essential for 60 S ribosomal subunit biogenesis. J Biol Chem **273:** 28912–28920

Griffith ME, Mayer U, Capron A, Ngo QA, Surendrarao A, McClinton R, Jurgens G, Sundaresan V (2007) The TORMOZ gene encodes a nucleolar protein required for regulated division planes and embryo development in *Arabidopsis*. Plant Cell **19:** 2246–2263

Groß-Hardt R, Kagi C, Baumann N, Moore JM, Baskar R, Gagliano WB, Jurgens G, Grossniklaus U (2007) *LACHESIS* restricts gametic cell fate in the female gametophyte of *Arabidopsis*. PLoS Biol **5:** e47

Grossniklaus U, Schneitz K (1998) The molecular and genetic basis of ovule and megagametophyte development. Semin Cell Dev Biol **9:** 227–238

Grossniklaus U, Vielle-Calzada J-P, Hoeppner MA, Gagliano WB (1998) Maternal control of embryogenesis by *MEDEA*, a polycomb group gene in *Arabidopsis*. Science **280:** 446–450

Hejatko J, Pernisova M, Eneva T, Palme K, Brzobohaty B (2003) The putative sensor histidine kinase CKI1 is involved in female gametophyte development in *Arabidopsis*. Mol Genet Genomics **269:** 443–453

Howden R, Park SK, Moore JM, Orme J, Grossniklaus U, Twell D (1998) Selection of T-DNA-tagged male and female gametophytic mutants by segregation distortion in *Arabidopsis*. Genetics **149:** 621–631

Johnson-Brousseau SA, McCormick S (2004) A compendium of methods useful for characterizing *Arabidopsis* pollen mutants and gametophytically-expressed genes. Plant J **39:** 761–775

Jorgensen P, Nishikawa JL, Breitkreutz BJ, Tyers M (2002) Systematic identification of pathways that couple cell growth and division in yeast. Science **297:** 395–400

Kim HU, Li Y, Huang AH (2005) Ubiquitous and endoplasmic reticulum-located lysophosphatidyl acyltransferase, LPAT2, is essential for female but not male gametophyte development in *Arabidopsis*. Plant Cell **17:** 1073–1089

Kwee HS, Sundaresan V (2003) The *NOMEGA* gene required for female gametophyte development encodes the putative APC6/CDC16 component of the anaphase promoting complex in *Arabidopsis*. Plant J **36:** 853–866

Lahmy S, Guilleminot J, Cheng CM, Bechtold N, Albert S, Pelletier G, Delseny M, Devic M (2004) DOMINO1, a member of a small plant-specific gene family, encodes a protein essential for nuclear and nucleolar functions. Plant J **39:** 809–820

Leon G, Holuigue L, Jordana X (2007) Mitochondrial complex II Is essential for gametophyte development in Arabidopsis. Plant Physiol **143:** 1534–1546

Leung AK, Andersen JS, Mann M, Lamond AI (2003) Bioinformatic analysis of the nucleolus. Biochem J **376:** 553–569

Liu M, Yuan L, Liu NY, Shi DQ, Liu J, Yang WC (2009) *GAMETOPHYTIC FACTOR1*, involved in pre-mRNA splicing, is essential for megagametogenesis and embryogenesis in Arabidopsis. J Integr Plant Biol **51:** 261–271

Liu YG, Mitsukawa N, Oosumi T, Whittier RF (1995) Efficient isolation and mapping of *Arabidopsis thaliana* T-DNA insert junctions by thermal asymmetric interlaced PCR. Plant J **8:** 457–463

Milkereit P, Gadal O, Podtelejnikov A, Trumtel S, Gas N, Petfalski E, Tollervey D, Mann M, Hurt E, Tschochner H (2001) Maturation and intranuclear transport of pre-ribosomes requires Noc proteins. Cell **105:** 499–509

Moll C, von Lyncker L, Zimmermann S, Kagi C, Baumann N, Twell D, Grossniklaus U, Gross-Hardt R (2008) CLO/GFA1 and ATO are novel regulators of gametic cell fate in plants. Plant J **56:** 913–921

Moore JM, Calzada JP, Gagliano W, Grossniklaus U (1997) Genetic characterization of *hadad*, a mutant disrupting female gametogenesis in *Arabidopsis thaliana*. Cold Spring Harb Symp Quant Biol **62:** 35–47

Pagnussat GC, Yu HJ, Ngo QA, Rajani S, Mayalagu S, Johnson CS, Capron A, Xie LF, Ye D, Sundaresan V (2005) Genetic and molecular identification of genes required for female gametophyte development and function in *Arabidopsis*. Development **132:** 603–614

Portereiko MF, Lloyd A, Steffen JG, Punwani JA, Otsuga D, Drews GN (2006a) AGL80 is required for central cell and endosperm development in *Arabidopsis*. Plant Cell **18:** 1862–1872

Portereiko MF, Sandaklie-Nikolova L, Lloyd A, Dever CA, Otsuga D, Drews GN (2006b) *NUCLEAR FUSION DEFECTIVE1* encodes the Arabidopsis RPL21M protein and is required for karyogamy during female gametophyte development and fertilization. Plant Physiol **141:** 957–965

Raška I, Koberna K, Malinsky J, Fidlerova H, Masata M (2004) The nucleolus and transcription of ribosomal genes. Biol Cell **96:** 579–594

Shaw P, Doonan J (2005) The nucleolus: playing by different rules? Cell Cycle **4:** 102–105

Sheridan WF, Huang BQ (1997) Nuclear behavior is defective in the maize (Zea mays L.) lethal ovule2 female gametophyte. Plant J **11:** 1029–1041

Shi DQ, Liu J, Xiang YH, Ye D, Sundaresan V, Yang WC (2005) *SLOW WALKER1*, essential for gametogenesis in *Arabidopsis*, encodes a WD40 protein involved in 18S ribosomal RNA biogenesis. Plant Cell **17:** 2340–2354

Smyth DR, Bowman JL, Meyerowitz EM (1990) Early flower development in *Arabidopsis*. Plant Cell **2:** 755–767

Springer PS, McCombie WR, Sundaresan V, Martienssen RA (1995) Gene trap tagging of *PROLIFERA*, an essential MCM2-3-5-like gene in *Arabidopsis*. Science **268:** 877–880

Srivastava M, Pollard HB (1999) Molecular dissection of nucleolin's role in growth and cell proliferation: new insights. FASEB J **13:** 1911–1922

Sundaresan V, Springer P, Volpe T, Haward S, Jones JD, Dean C, Ma H, Martienssen R (1995) Patterns of gene action in plant development revealed by enhancer trap and gene trap transposable elements. Genes Dev **9:** 1797–1810

Wade C, Shea KA, Jensen RV, McAlear MA (2001) EBP2 is a member of the yeast RRB regulon, a transcriptionally coregulated set of genes that are required for ribosome and rRNA biosynthesis. Mol Cell Biol **21:** 8638–8650

Warner JR, Vilardell J, Sohn JH (2001) Economics of ribosome biosynthesis. Cold Spring Harb Symp Quant Biol **66:** 567–574

Wilson ZA, Yang C (2004) Plant gametogenesis: conservation and contrasts in development. Reproduction **128:** 483–492

Wullischleger S, Loewith R, Hall MN (2006) TOR signaling in growth and metabolism. Cell **124:** 471–484

Xie Q, Sanz-Burgos AP, Guo H, Garcia JA, Gutierrez C (1999) GRAB proteins, novel members of the NAC domain family, isolated by their interaction with a geminivirus protein. Plant Mol Biol **39:** 647–656

Yagi N, Takeda S, Matsumoto N, Okada K (2009) VAJ/GFA1/CLO is involved in the directional control of floral organ growth. Plant Cell Physiol **50:** 515–527

Yang WC, Sundaresan V (2000) Genetics of gametophyte biogenesis in *Arabidopsis*. Curr Opin Plant Biol **3:** 53–57

Yang WC, Ye D, Xu J, Sundaresan V (1999) The *SPOROCYTELESS* gene of *Arabidopsis* is required for initiation of sporogenesis and encodes a novel nuclear protein. Genes Dev **13:** 2108–2117

Zhang Y, Yu Z, Fu X, Liang C (2002) Noc3p, a bHLH protein, plays an integral role in the initiation of DNA replication in budding yeast. Cell **109:** 849–860

Zimmermann P, Hirsch-Hoffmann M, Hennig L, Gruissem W (2004) GENEVESTIGATOR. Arabidopsis microarray database and analysis toolbox. Plant Physiol **136:** 2621–2632